# Predictive Computational Fluid Dynamics Simulation of Fire Spread on Wood Cribs

*R. Kallada Janardhan and S. Hostikka\** (ID) , *Aalto University, Espoo, Finland*

***Abstract.*** Presently, there is a need for a robust numerical simulation approach to investigate the influence of various parameters on fire spread in large open framed structures. CFD-based methods can already be used for analyzing the fire conditions but they are difficult to apply for large calculations where the geometrical details of the fuel are sub-grid scale. In this paper we present a CFD-based fire spread simulation method that makes use of the ignition temperature model for pyrolysis and introduce a correction for the mesh dependency of the fuel surface area. Wood sticks, with an ignition temperature of 300°C and a specified heat release rate per unit area of 260 kW/m$^2$, were used as fire load. The method was validated using laboratory scale tunnel (10 m $\times$ 0.6 m $\times$ 0.396 m) fire tests with a longitudinal velocity of 0.6 m/s, demonstrating a 3% bias for the peak heat release rates and less than 33% biases for the fire growth rate. The method was then applied to room-scale fire spread simulations with uniformly distributed wood cribs at 600 MJ/m$^2$. The results show that, with the help of the surface area correction, the fine-mesh predictions of the heat release rate and thermal environment can be reproduced with coarser meshes and one order of magnitude lower computational costs. Due to the inherent inability of the large-scale CFD to resolve the flame temperature, there is a minimum size of the initial, prescribed fire area which is required for consistent fire spread predictions. Through this study, the authors attempt to build a reliable CFD modelling approach for fire spread and traveling fires.

## 1. Introduction

Structural design for fire resistance of most large compartments is still based on the results obtained from the standardized tests with spatially homogeneous temperature field. Standard time-temperature fire curves were developed based on large scale furnace tests conducted for vertically loaded steel, reinforced concrete, cast iron and timber columns [1]. The temperature gradient experienced in these furnaces was relatively low in comparison to real fire scenarios.

Petterson and Magnusson [2] developed a set of time-temperature fire curves which consider the effects of ventilation, fuel load and compartment linings. This work was later used to develop the parametric temperature-time curve in the Eurocode-1, applicable only to fire compartments with floor areas up-to 500 m$^2$

---

\* Correspondence should be addressed to: S. Hostikka, E-mail: simo.hostikka@aalto.fi

without roof openings and with a maximum height of 4 m [3]. This restriction rules out almost all the modern large, open frame buildings. With time, many other methods which provided temperature-time curves for fire resistance analysis were developed [4–6]. All these methods however make the same assumption that the fires induce uniform heating loads on the structures. Development of the natural fire concept during the early 2000s was an attempt at describing a realistic fire safety concept where fire spread, ventilation and compartment linings are accounted. The full scale fire tests carried out at Cardington with uniformly spaced wood cribs demonstrated the variation between temperature curves of the Eurocodes and a realistic design basis for fires [7].

In 2012, Stern-Gottfried and Rein proposed the concept of travelling fires for fire engineering design of large compartments [8, 9]. In a travelling fire, a localised fire would propagate through the compartment depending on the availability of fuel and oxygen. This idea contradicts the often used fire resistance testing process assumption of uniform heating loads on structural elements. Temperature gradients experienced in a travelling fire are variable over time and space. The stresses induced by this type of heating process can be more detrimental to the structure than a standard fire. Since the introduction of this concept, there have only been a few large scale experiments conducted and little information of such fires currently exist [10, 13]. This is where computational fluid dynamics (CFD) based models can be used to understand the behaviour of large scale fires, but this task presents additional challenges from the modelling perspective as well.

Fire spread is a difficult problem to accurately simulate because of the different time and length scales involved. Based on the length scales we can identify three categories of fire spread simulations (see Fig. 1): (1) Flame spread simulations where the flames and surfaces are well resolved. Here the aim is to resolve the boundary layer flows. (2) Room scale fires where flames and surfaces are partially resolved. In these simulations, the flame features are not resolved and fuel geometry is simplified. (3) In wild-land fire simulations, each computational cell spans a few metres or tens of metres. Fuel surface is not resolved and is modelled using sub-grid scale models. The scale of interest in our case is the partially resolved room scale fires.



Well resolved fire          Partially resolved          Highly coarse
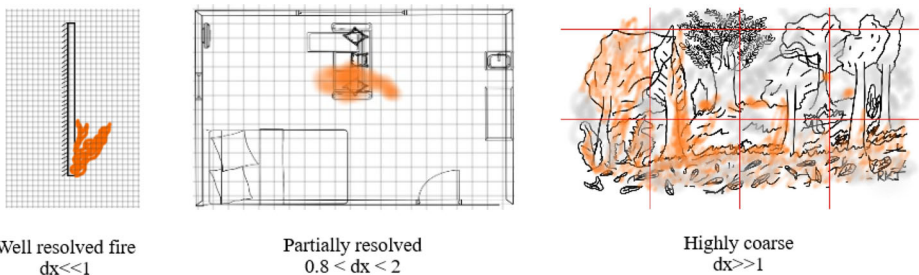    dx<<1                     0.8 < dx < 2                  dx>>1

**Figure 1. A comparison of different simulation scales—flame spread scenario with high resolution, compartment fire with moderate resolution and highly coarse wildfire scenario.**

Fire spread modelling started with deterministic mathematical models [14] and progressed to probabilistic and stochastic models like the ones proposed by Ling and Williamson [15], Ramachandran [16], Platt et al. [17], Cheng and Hadjisophocleus [18] and many more. These models though are usually one dimensional and cannot model the fire spread process in detail. Recent advancement of computers allowed the use of CFD models to predict fire behaviour inside large compartments. Bryner et al. [19] reconstructed the initial 300 s of growth and spread of the Station Nightclub fire that occurred in Rhode Island, USA using Fire Dynamics Simulator (FDS) and reported that the model predictions were consistent with the observations. Initial fire was prescribed for 30 s and then the fire was allowed to spread by assigning an ignition temperature to combustibles in the building. Galea et al. [20] used multiple fire simulation tools to extend the nightclub fire study to include an enhanced flame spread, toxicity and evacuation. Fire spread in this study was modelled using a combination of an ignition temperature and a critical heat flux. Chen et al. [21] tried to reproduce the results of a furnished office fire experiment in FDS using a prescribed heat release rate (HRR) behaviour. They concluded that a grid size of 5 cm produced the best results when the default extinction model parameters were adjusted. Yang et al. [22] studied the fire spread in storehouse shelves using pallets of wood by prescribing the heat release rate per unit area (HRRPUA). Ahn and Kim [23] simulated predictive fire spread across an entire building floor. They concluded that the simulations underestimated temperature by 20% and its temporal evolution was delayed by 15% in comparison to the experiments. Shu et al. [24] studied the influence of stack effect caused by different patio lengths on fire spread using numerical simulations. Chi [25] used FDS to reconstruct a fire that occurred in a Taiwanese hotel by prescribing the HRR and spread rate values for fire. Meunders et al. [26] used optimized kinetic properties of PU foam from small scale experiments to predict fire spread from an ignitor to a PU foam armchair and reported good reproduction of PU decomposition behaviour. Comparison to experiments showed that the simulations reproduced the fire growth and spread process. Grid sensitivity analysis showed that a 5 cm grid was able to produce the best results. All these simulations had their own set of limitations. The fuel behaviour was mostly prescribed or they were reconstructions of fire scenarios where accuracy of the initial data is low. The simulations mostly used fine meshes ($\approx$ 5 cm) which are not computationally feasible for engineering applications and the computational times were not reported. Simulation of fire spread would require a simplified yet reliable pyrolysis model and a method to improve computational efficiency.

Pyrolysis of the fuel can be simplified by using the ignition temperature criterion for combustibles. Employing coarse meshes can reduce computational time but this reduces predictive accuracy as well. Coarse meshes decrease the available burning surface area as the geometry is simplified and results in the loss of numerical accuracy in solving the gas phase scalar and vector fields. The change in geometry of fire load alters the heat transfer characteristics significantly. The surface area of fuel object in a coarse mesh is usually lower than in a fine mesh and to solve this problem, we introduced a simple multiplication factor called Area Adjust in FDS. This parameter artificially increases the mass flux of fuel from a

surface by multiplying it with the specified area adjust value. A similar parameter like this was used by Cheong et al. [27] to simulate the Runehamar tunnel fire tests in which a trailer containing various types of fuels was used as fire load. The authors in [27] used a surface burning factor to calibrate the HRR by adjusting the HRRPUA, thus accounting for the surface area inaccuracy in coarse mesh. Our study differentiates itself from the previous study by focussing on prediction of fire spread and addressing the issue of grid dependence for future applications as well.

The objective of this study is twofold, one is to validate the use of ignition temperature model accompanied by area adjust for coarse mesh fire spread simulations. Experiments conducted by Hansen and Ingason [28, 29] serve as test cases for validation simulations. The second objective is to perform room scale fire spread calculations reliably. Ideally, the ignition for fire spread would be modelled from a small source but with mesh resolutions used in typical engineering applications this is not possible as the ignition source is not sufficiently resolved to cause fire spread. Our hypothesis is that to perform a room scale simulation with consistent fire spread, a certain area of initial prescribed fire would be required. This hypothesis is tested in a room with uniformly distributed fire load.

## 2. Methods

### 2.1. Numerical Method

Fire dynamics simulator (FDS) is a large eddy simulation (LES) based computational fluid dynamics software which solves the low Mach number combustion equations on a rectilinear grid over time [30]. The simulations in this study were performed using FDS version 6.6.0. Combustion is handled by a turbulent batch reactor model based on the Eddy dissipation concept in which the mixing of fuel and oxygen is a single step reaction. Eddy viscosity is modelled using Deardoff model, the default turbulence model in FDS and the near-wall eddy viscosity was handled using the Smagorinsky model with Van Driest damping [31].

Wood cribs are used as fuel for all the simulations in this paper. The one dimensional heat conduction equation is used to solve heat transfer within a solid obstruction. The gas phase temperature and heat flux on the front and back side serve as boundary conditions. Here $\rho_s, k_s, c_s$ are the density, conductivity and specific heat of the solid, respectively.

$$\rho_s c_s \frac{\partial T_s}{\partial t} = \frac{\partial}{\partial x}\left(k_s \frac{\partial T_s}{\partial x}\right) \tag{1}$$

Ignition of fuel object occurs when the temperature of a surface cell reaches a specified value. The fuel mass flux is then controlled by a user specified heat release behaviour.

Conservation of mass in the simulations is ensured using a bulk density value for each cell containing fire load. The fuel mass in a cell is then determined as a

product of the bulk density and cell volume. A fuel containing cell is changed into a gas phase cell when Eq. 2 is satisfied.

$$\int_o^t \dot{m}_f'' A_{cell} dt > \rho_{bulk} V_{cell} \tag{2}$$

Fuel surfaces in coarse meshes cannot be resolved as accurately as in the fine mesh simulations and this results in a reduction of surface area in coarse meshes. A multiplication factor called area adjust ($\phi$) is used to maintain the same fuel surface area between fine and coarse meshes. This factor multiplies the mass flux of a cell by the specified area adjust value. Activation of burn away when area adjust is used occurs when Eq. 3 is satisfied. The bulk density used in coarse meshes is usually different from the one used in the fine mesh simulations.

$$\int_o^t \phi \dot{m}_f'' A_{cell} dt > \rho_{bulk} V_{cell} \tag{3}$$

## 2.2. Validation: Ignition Temperature Model

Validation simulations were performed using the tunnel fire experiments of SP, Sweden [28]. The tests were conducted in a laboratory scale tunnel to study the influence of fuel objects placed at varying distances on the total HRR under the effect of ventilation. Altogether, 12 tests were carried out in a tunnel of dimensions 10.0 m $\times$ 0.6 m $\times$ 0.4 m with piles of white pine wood pallets as fuel load. The parameters tested were the distance between piles of wood pallets and longitudinal ventilation velocities ($u_c$). Four piles of pallets were used and their arrangement is as shown in Fig. 2a. The boundaries were made from Promatect-H board whose properties are specified in Table 2. Test 1, 4 and 12 were reference tests performed with a single pile. Gas temperatures were measured with a 0.25 mm K type thermocouples at a height of 0.36 m. The description of tests carried
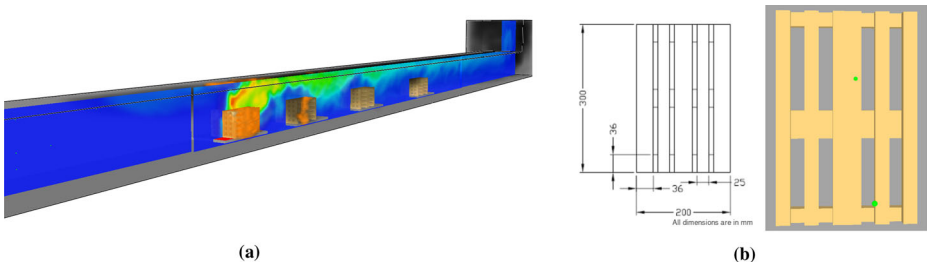


(a)        (b)

**Figure 2.** **(a) Simulated model of the tunnel with piles of wood pallets. (b) Comparison of the wood pallet used in experiments (left) and the pallet used in fine-mesh simulations (right). Figure taken from report by Hansen and Ingason [29].**

out is given in Table 1. In this work, we used only the tests with 0.6 m/s velocity (Tests 3–11) to minimize the uncertainty due to the exhaust arrangement.

*2.2.1. Simulation Model* The spatial resolution used in the first set of validation simulations was 2 cm × 2 cm × 1.8 cm in X,Y and Z directions, allowing for an accurate reproduction of wood pallet surface area. The connecting meshes have a resolution of 4 cm × 4 cm × 1.8 cm in X,Y and Z directions. Simulations with multiple wood piles used 8 meshes and each mesh was assigned to a single MPI process.

The experimental tunnel was modelled as per dimensions 10.9 m × 0.6 m × 0.4 m. Tunnel inlet boundary condition(BC) was modelled as a supply vent with a fixed velocity of 0.6 m/s and outlet BC as a HVAC duct connected to the ambient. Exhaust system was not modelled as per experiments because its performance parameters were not available. The heat release rate per unit area (HRRPUA) of the wood and ignitor properties (HRRPUA and duration) were determined through the inverse modelling of tests 1 and 4.

*2.2.2. Fuel Geometry* The wood pallet was modelled as collection of wood sticks. It was ensured that the simulated pallets resembled the experiments closely. Each pile consisted of three types of sticks with different dimensions: Type 1: 0.3 m × 0.02 m × 0.018 m, Type 2: 0.2 m × 0.02 m × 0.018 m, and Type 3: 0.2 m × 0.04 m × 0.036 m. Each pile in the simulation consisted of 5 pallets. Figure 2b shows a comparison of the experimental and simulated wood pallet.

*2.2.3. Fuel Specifications* The fuel in FDS was defined by the formula $C_{3.4}H_{6.2}O_{2.5}$ and was assigned a critical flame temperature of 1337°C [34] which means that a

**Table 1**
**Distance Between Pallets and Ventilation Velocity Used in the SP Tunnel Fire Experiments**

| Test no. | $u_c$ (m/s) | Distance between piles | | |
| --- | --- | --- | --- | --- |
| | | Pile 1–Pile 2 | Pile 2–Pile 3 | Pile 3–Pile 4 |
| 1 | 0.3 | – | – | – |
| 2 | 0.3 | 0.6 | 0.9 | 0.9 |
| 3 | 0.6 | 0.4 | 0.7 | 0.6 |
| 4 | 0.6 | – | – | – |
| 5 | 0.6 | 0.5 | 0.7 | 0.8 |
| 6 | 0.6 | 0.5 | 0.8 | 0.9 |
| 7 | 0.6 | 0.5 | 0.8 | 1.1 |
| 8 | 0.6 | 0.5 | 0.8 | 1.3 |
| 9 | 0.6 | 0.6 | 0.8 | 1.1 |
| 10 | 0.6 | 0.7 | 0.8 | 1.1 |
| 11 | 0.6 | 0.7 | 0.9 | 1.1 |
| 12 | 0.9 | – | – | – |

mixture of fuel and air in a cell must be able to produce the assigned temperature value. For the fuel gas properties, those of ethylene were used, including the radiative fraction of 0.35 and soot yield of 0.01. The reported values for heat of combustion, 18,100 kJ/Kg K, was used in the simulations as well. Ignition temperature of the fuel was chosen to be 300°C based on the values of white pine used by Hietaniemi et al. [33]. The uncertainty associated with the ignition temperature value is not known.

For the wood sticks, the HRRPUA was maintained at a constant value of 260 kW/m$^2$ and the burnout of fuel was modelled using Eq. 2. This value of HRRPUA was obtained based on the simulation of Reference test 4 described in Table 1. Wood material thickness was set to 0.036 m, corresponding to the thickest part of the experimental pallet. The burn away and bulk density parameters in FDS were used to ensure the correct total combustible mass. The burn away parameter attempts to model the mass loss of the pallet but introduces an unrealistic behaviour during the extinction phase. The properties of wood were taken from correlations in [11], and summarized in Table 2.

Ignition in the experiments was achieved using a small cube of fibreboard, 0.03 m × 0.03 m, soaked in heptane. In the simulations, a larger ignitor size, 0.1 m × 0.1 m, was chosen so that a better flame resolution can be achieved. HRR of the ignitor was controlled to yield a behaviour similar to the experiments. Optimum HRRPUA of the ignitor was found to be 750 kW/m$^2$. Maximum value of HRR is attained in 42 s and is sustained for 23 s until it extinguishes at 80 s.

## 2.3. Validation: Area Adjust Parameter

The validation simulations with a fine mesh were computationally expensive to perform. Using a coarse mesh would reduce the computational time. At the same time, the pallet geometry is changed and the surface area reduced which affects the total burning rate. The capability of the Area adjust parameter to compensate for the reduced surface area was tested in three configurations of coarser meshes. Figure 3 shows the pallet geometries and the details of the configurations are given in Table 3. In Configuration 1, the mesh containing the ignition pile (Initial

**Table 2**
**Properties of Wooden Fuel Used**

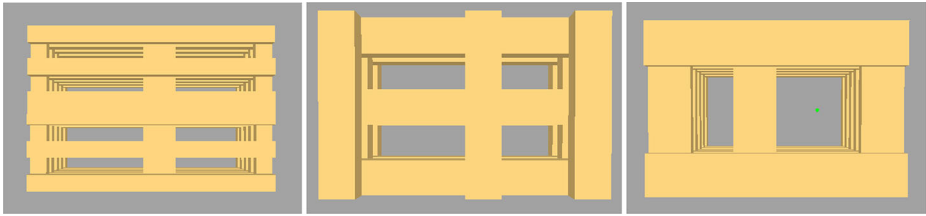| Material | Ignition temperature (°C) | k (W/m$^2$/s) | Cp (kJ/kg K) | $\rho$, kg/m$^3$ | Moisture (%) | HRR ramp |
|---|---|---|---|---|---|---|
| Pine | 300 | 0.11 | 1.35 | 370 | 5 | T = 0, H = 0 <br> T = 15, H = 1 <br> T = 50, H = 1 <br> T = 60, H = 0.85 |
| Promatect-H | – | 0.175 | 1.13 | 870 | – | – |

**Figure 3. Pile geometries in 2 cm, 4 cm and 5 cm grid resolutions respectively. The geometry of the pile changes with increasing mesh size.**

fire mesh) was sufficiently fine to retain the correct surface area of the pile ($0.8704\,\mathrm{m}^2$). The downstream meshes were coarser, and the pallets within them were built of sticks $0.3 \times 0.04 \times 0.036$ m$^3$ and $0.2 \times 0.04 \times 0.036$ m$^3$ The surface area of these piles was $0.5904\,\mathrm{m}^2$, i.e. 47% lower than reality. Consequently, the area adjust parameter for Configuration 1 was $0.8704/0.5904 \approx 1.47$. In configurations 2 and 3, the surface areas were reduced in all meshes by 47% and 20%, respectively.

## 3. Validation Results

The tunnel fire simulations with the fine mesh were run on the CSC-Taito supercomputer over multiple nodes. The simulations used 8 meshes and each mesh was assigned to a single MPI process. Each simulation used approximately 220,000 computational cells and CPU time for the fine-mesh simulations varied between 56 and 72 h. The results of the heat release rates in the fine-mesh simulations are illustrated in Fig. 4, allowing us to compare the peak heat release rates and fire growth times, defined as the time to reach a HRR of 350 kW.

The HRR predictions with a fine mesh show good agreement with the experiments. The predicted peak heat release rates were in average 99% of the measured ones, and the fire growth times were in average 92% of the measured times. The largest differences in the fire growth times are observed in tests 10 and 11 where

**Table 3**
**The Mesh Resolutions (cm) and Area Adjust Parameters $\phi$ for the Three Validation Configurations**

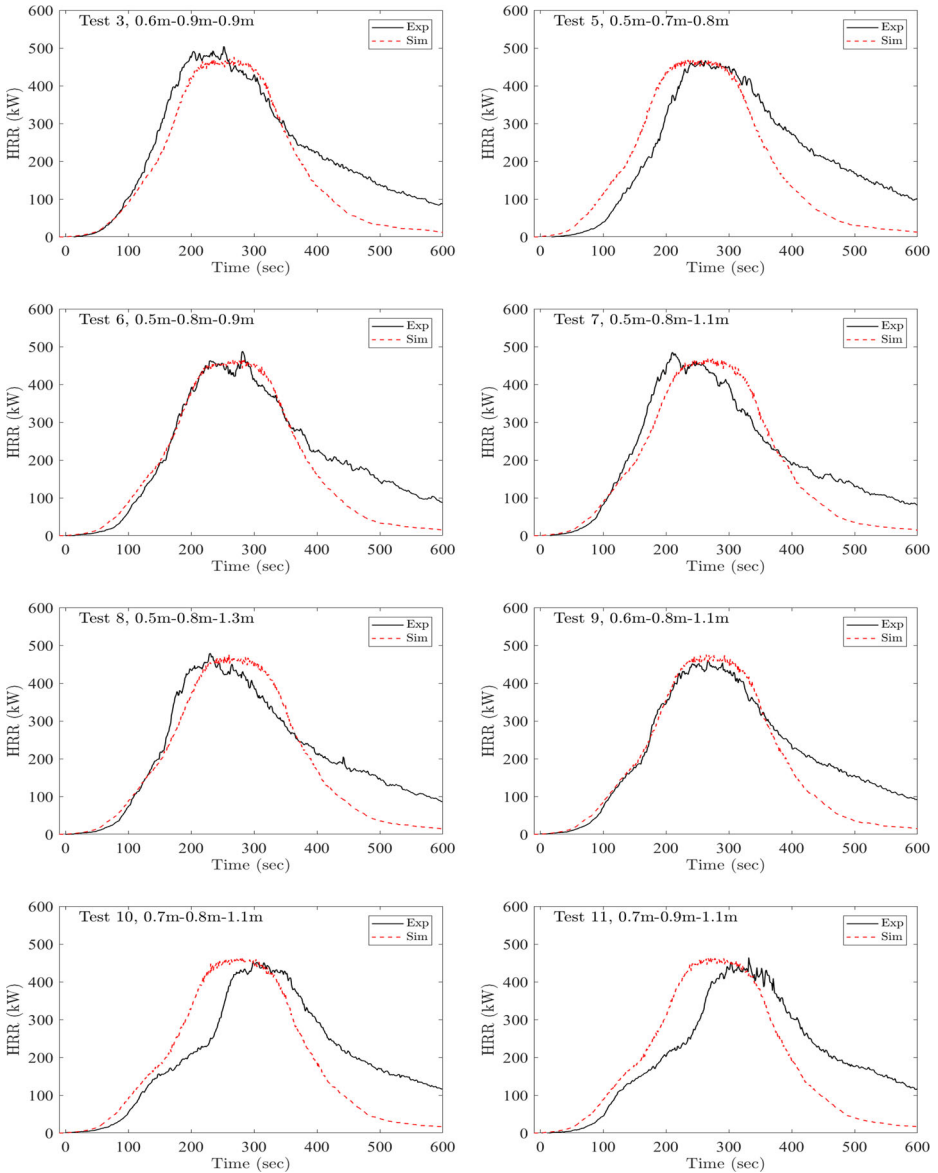|  | Initial fire mesh | | | | Downstream meshes | | | |
|---|---|---|---|---|---|---|---|---|
|  | X | Y | Z | $\phi$ | X | Y | Z | $\phi$ |
| Configuration 1 | 2 | 2 | 1.8 | 1 | 4 | 4 | 3.6 | 1.47 |
| Configuration 2 | 4 | 4 | 3.6 | 1.47 | 4 | 4 | 3.6 | 1.47 |
| Configuration 3 | 5 | 5 | 1.8 | 1.2 | 5 | 5 | 1.8 | 1.2 |

**Figure 4. Comparison of experimental and simulated fine-mesh HRR. Distance between pallets in each test are indicated in the plot titles.**

the distance between piles was increased. In the decay phase, HRR is under-predicted as the processes of char retention and glowing are difficult to model with the ignition temperature and the burn away concept.

The performance of the area adjust correction was validated in Tests 3, 6 and 9 using three different mesh configurations, listed in Table 3. These simulations used

8 meshes and each mesh was assigned to a single MPI process. The runtimes varied between 12 and 30 h, depending on the mesh resolution.

The results of the validation simulations using area adjust are presented in Figs. 5, 6 ad 7 together with fine mesh and uncorrected coarse mesh simulations ($\phi = 1$). The results of the coarse mesh simulations without area adjustment show significantly under-predicted peak HRR in all cases, being more significant for configurations 2 and 3. Area adjustment improves the peak HRR predictions, making them almost independent of the mesh. With area adjustment, the HRR curves are found to plateau during the period of maximum burning rate.

In coarse mesh simulations without area adjust, a temporal delay in the fire growth rate is observed in configurations 2 and 3, i.e. the simulations where the initial fire mesh was coarse. The long delay in Configuration 3 may have been caused by the cell aspect ratio 2.77 which is higher than the recommended maximum of 2 [31]. With area adjust, the coarse-mesh predictions of fire growth time in configurations 1 and 2 are 13% and 33% faster than the fine-mesh predictions, respectively, and 22% slower in Configuration 3.

Overall, the area adjust correction significantly improves both the peak HRR and the fire growth predictions in comparison to uncorrected simulations. The actual efficiency depends, to some extent, on the size and quality of the coarse mesh. These results demonstrate that the problems of the CFD-based fire spread predictions, reported frequently in the fire research literature, may have been caused by the non-conservative description of the fuel surface area.
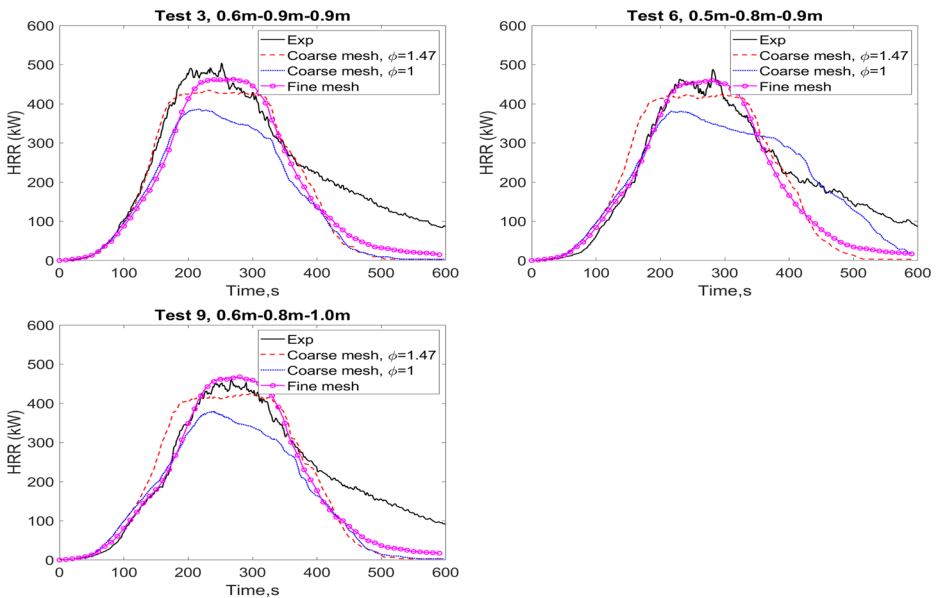


**Figure 5. Area adjust validation results for the total HRR in Configuration 1: doubled cell size in downstream meshes.**
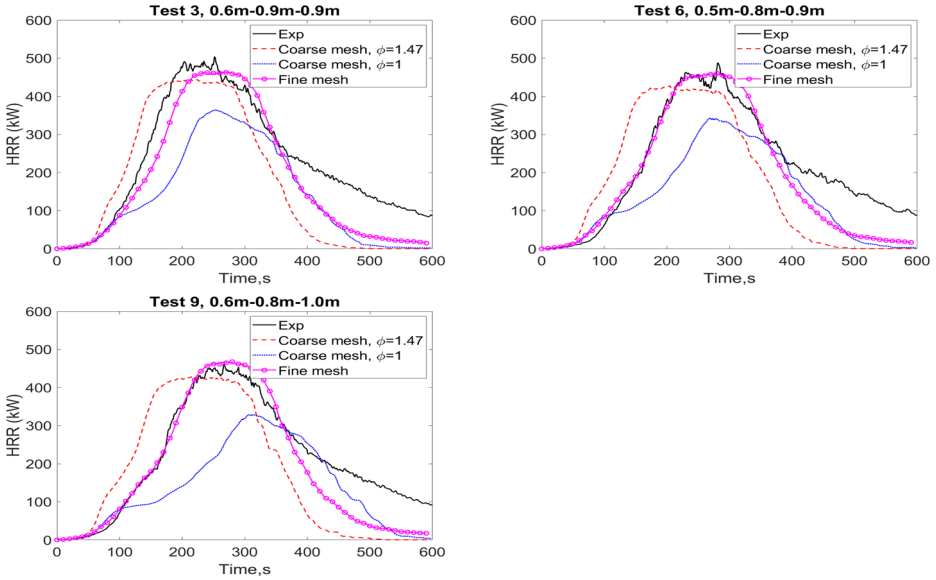
**Figure 6.  Area adjust validation results for the total HRR in Configuration 2: doubled cell size in all the meshes.**
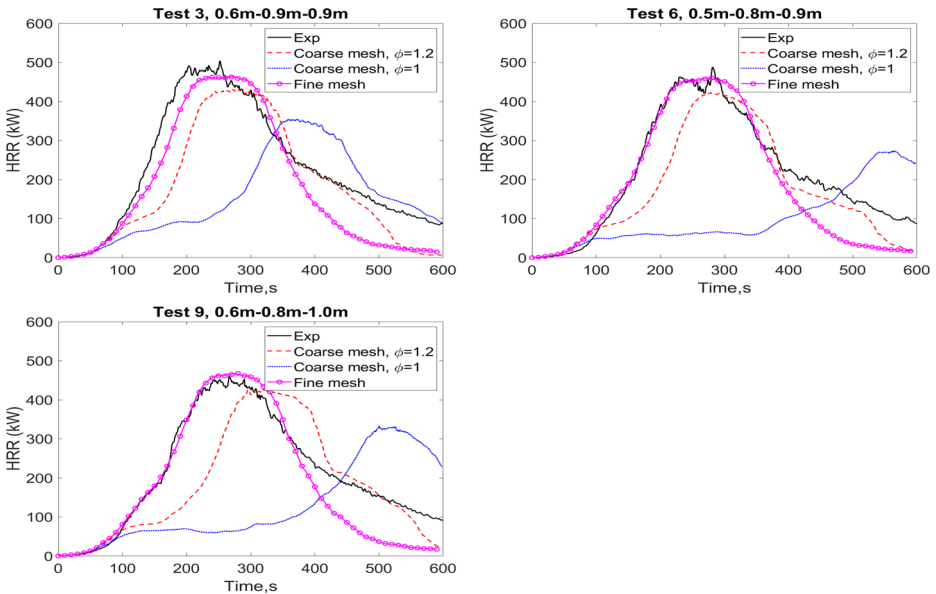


**Figure 7.  Area adjust validation results for the total HRR in Configuration 3: 2.5 times larger cells horizontally in all meshes.**
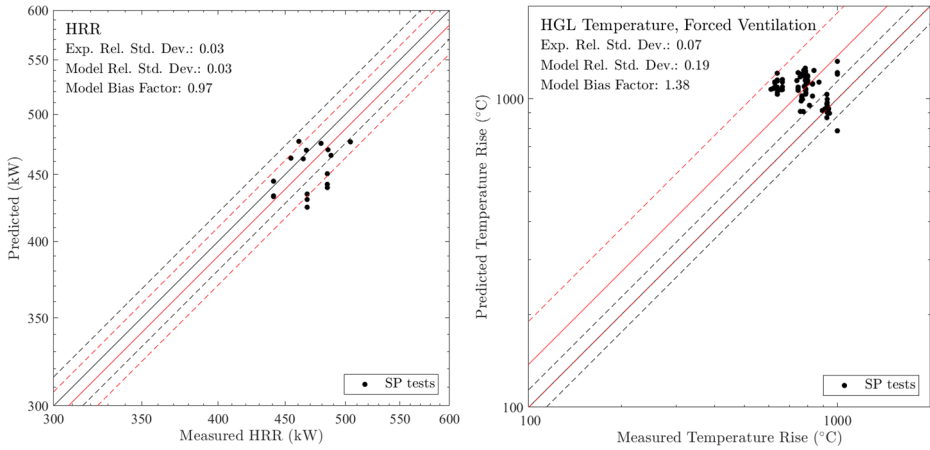
**Figure 8.  Combined scatter plots of heat release rates and gas temperatures for the validation simulations.**

Combined scatter-plots of the peak HRR and gas temperatures for the fine-mesh and area adjusted validation simulations are shown in Fig. 8. In average, the validation simulations under-predict the peak HRR by 3% and over-predict temperatures by 38%. The random deviations between the measured and simulated gas temperatures are much higher than between the global HRR values. A detailed analysis of the temperature data revealed that while the measured temperatures varied between the tests with different pile spacing, the predicted temperatures remained almost unchanged. As the simulation domain is a longitudinally ventilated tunnel, the hot gases flow downstream and cause the ignition of downstream wood cribs. The lack of gas temperature dependence thus explains the too fast fire growth in tests 10 and 11 simulations. Temperature over-prediction does not affect the peak HRR as the HRRPUA value was calibrated based on single crib tests.

Table 4 summarizes the model bias and relative standard deviation for the peak HRR in fine-mesh, non-adjusted and area adjusted simulations.

**Table 4**
**Summary of the Model Bias and Standard Deviations of Peak HRR for the Fine-Mesh and Coarse Mesh Configurations**

|                 | No area adjust |             | Area adjust |             |                     |
|-----------------|----------------|-------------|-------------|-------------|---------------------|
|                 | Bias           | Rel.Std.Dev | Bias        | Rel.Std.Dev | Average CPU time (h) |
| Fine-mesh       | 0.99           | 0.02        | –           | –           | 64.3                |
| Configuration 1 | 0.84           | –           | 0.94        | –           | 26.1                |
| Configuration 2 | 0.75           | –           | 0.95        | –           | 13.3                |
| Configuration 3 | 0.71           | –           | 0.94        | –           | 11.8                |

# 4. Compartment Fire Spread Simulations

## 4.1. Model Description

In order to study the capability of the area adjust parameter in reducing the grid dependency for a large scale application, fire spread was simulated in a compartment with uniformly distributed fire load. The dimensions of the simulated compartment were 30 m × 30 m × 3.6 m. Compartment boundaries were specified as open surfaces to ensure that ventilation does not influence fire spread. Generic concrete properties were specified for the floor and ceiling surfaces [36].

The simulation domain was decomposed into 9 to 16 meshes depending on the grid resolution employed. The span of each mesh was 10 m × 10 m as shown in Fig. 9b. Three different mesh resolutions—5 cm, 10 cm and 20 cm—were used for the central mesh, and the resolution of the other meshes was 20 cm. In the simulation with 5 cm resolution, the central mesh had to be further divided into smaller meshes.

The fire load was a uniform crib across the entire floor area, made up of 30 m long sticks. The height of the crib was kept constant (0.4 m) but as the number of sticks and layers changed with the mesh resolution the bulk density parameter was used to maintain the fire load density of 600 MJ/m$^2$. The thickness and width of wood sticks was equal to the mesh cell size. Properties of wood was identical to those described in Table 2 except that the burning behaviour (HRR ramp) was not specified here.

Fire spread was modelled using a combination of prescriptive and predictive modelling methods. An initial area of fire (red region in Fig. 9a) was prescribed at the centre of the compartment. Within the initial area of fire, an ultra-fast fire growth was specified with HRR reaching 1 MW in approximately 75 s. Spread rates were calibrated to achieve the desired growth rate, being 0.00533 m/s, 0.00693 m/s and 0.0071 m/s for the 5 cm, 10 cm and 20 cm resolutions, respectively. Three different prescribed areas were used in the simulations—4 m$^2$, 16 m$^2$
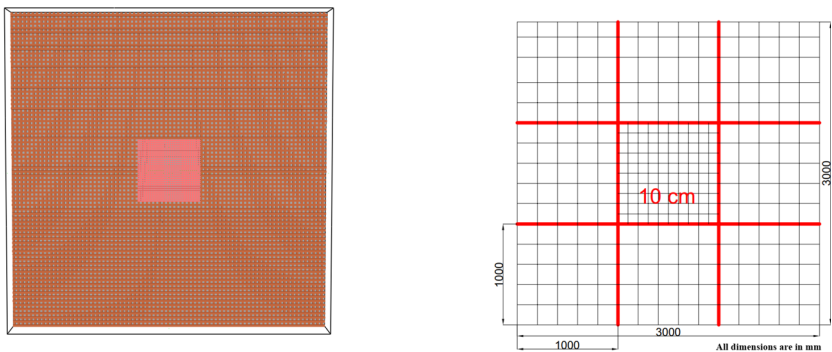


(a) Compartment with a uniformly distributed fire load of 600 MJ/m$^2$

(b) Mesh layout of the compartment.

**Figure 9. Compartment model with fire load and mesh layout used in the 10 cm grid simulations.**

and 36 m$^2$. Around the prescribed area, a predictive region based on the 300°C ignition temperature was used. The bulk density and burn away parameters described in Sect. 2.1 were used in these simulations as well. For the 5 cm grid resolution, fire spread was simulated only with prescribed areas of 4 m$^2$ and 16 m$^2$ due to the limited computational resources.

## 4.2. Results

Room scale fire spread simulations were performed using the CSC-Taito super-computer. The 5 cm simulations took 6 days to complete 160 s of fire spread. The 10 cm and 20 cm grid simulations took between 24–64 and 6-12 h respectively, to simulate 600 s of fire spread.

The evolution of fire spread in the compartment is illustrated in Fig. 10. Fire spread starts at the prescribed rate from the compartment centre and spreads evenly towards the predicted region. In simulations with prescribed areas of 16 m$^2$ and 36 m$^2$, the predicted fire load starts burning before the prescribed fire reaches it. This leads to an asymmetric fire spread across the compartment. By the end of the runtime, fire load starts to disappear as the all fuel in the cells is consumed.

The predicted HRR from the simulations with 5 cm and 10 cm resolutions without area adjust correction are compared in Fig. 11. The 10 cm calculations are found to replicate the HRR evolution of 5 cm simulations without using an area adjust factor, and they are thus used as a reference for the 20 cm simulations below. However, as the 5 cm simulations could not be run beyond 160 s, it is unknown if the results would be convergent after this time.

Figure 12 shows the performance of coarse mesh (20 cm) simulations with the 10 cm simulation results as the reference. The results show that the 20 cm grid resolution with $\phi = 1.0$ produces significantly slower HRR growth than the 10 cm grid. Area adjustment $\phi = 1.66$ improves the HRR predictions of 20 cm grids significantly except for the case with a prescribed area of 4 m$^2$. This indicates that the size of the prescribed fire also influences the fire spread predictions.

The estimated model bias for the heat release rate predictions, based on the SP tests was 3%. This was obtained from as precise modelling of the experiments as practically possible. In room scale simulations, the uncertainty can be significantly higher. The lower bound of the simulation uncertainty is given by the experimental uncertainty, which for HRR measurements in ventilated room fires has been estimated to be 11% [12]. On the other hand, according to the FDS Validation Guide, the relative model standard deviation for the burning rate predictions is 35% [32].

Temperatures in the compartment were recorded 20 cm below the ceiling and net heat fluxes at the top of the fire load, i.e. 0.4 m from the floor. Average temperatures and net heat fluxes in the compartment are plotted in Fig. 13. Despite the area adjustment, the 20 cm resolution leads to lower temperatures and net heat fluxes in comparison to 10 cm grid. The difference between the results decreases as area of the prescribed fire increases from 4 m$^2$ to 16 m$^2$ and to 36 m$^2$. The shaded region indicates the time after which the flames start to burn at the
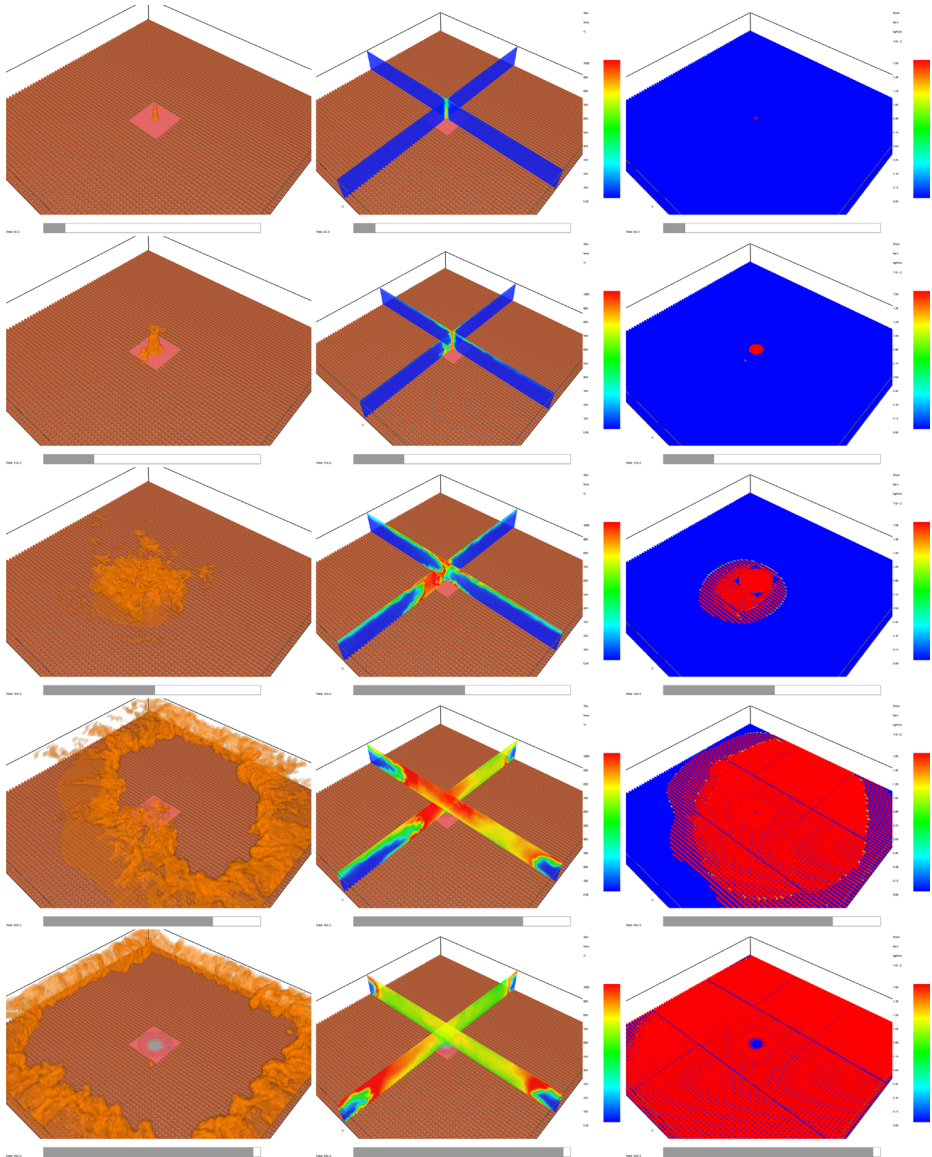
**Figure 10.** Illustration of fire spread development within the compartment with each row corresponding to a particular time. The start of fire spread in the prescribed region (row 1) to its spread to the predicted region (row 3) and across the entire compartment (row 6) is presented. Images in column 2 and column 3 also illustrates the temperature slices and burning rate respectively.
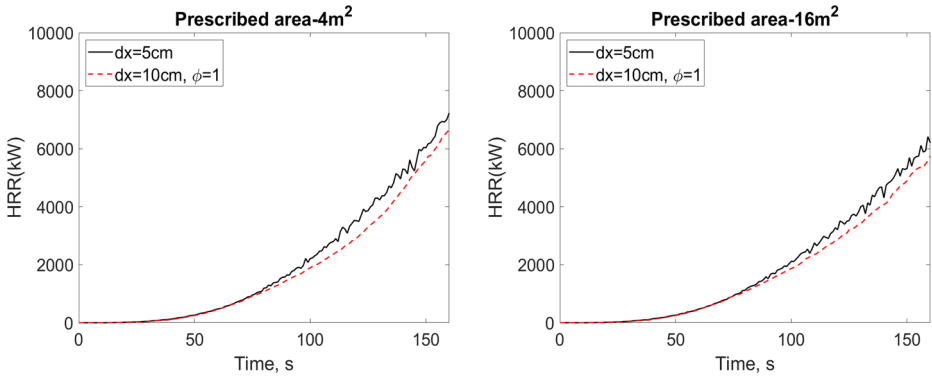
**Figure 11.** HRR results for simulations with prescribed areas of 4 m² and 16 m² with 5 cm and 10 cm grid resolutions without area adjust.
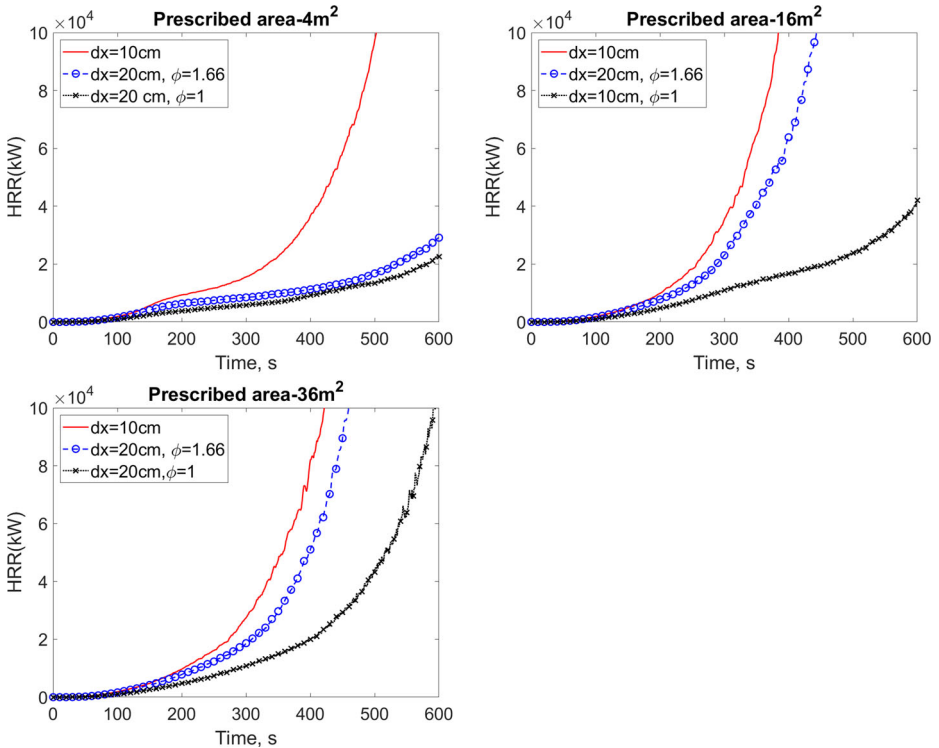


**Figure 12.** Predicted HRR in the compartment for the prescribed areas 4 m², 16 m² and 36 m² with 10 cm and 20 cm mesh resolutions. 20 cm results are given without ($\phi = 1$) and with area adjust ($\phi = 1.66$).
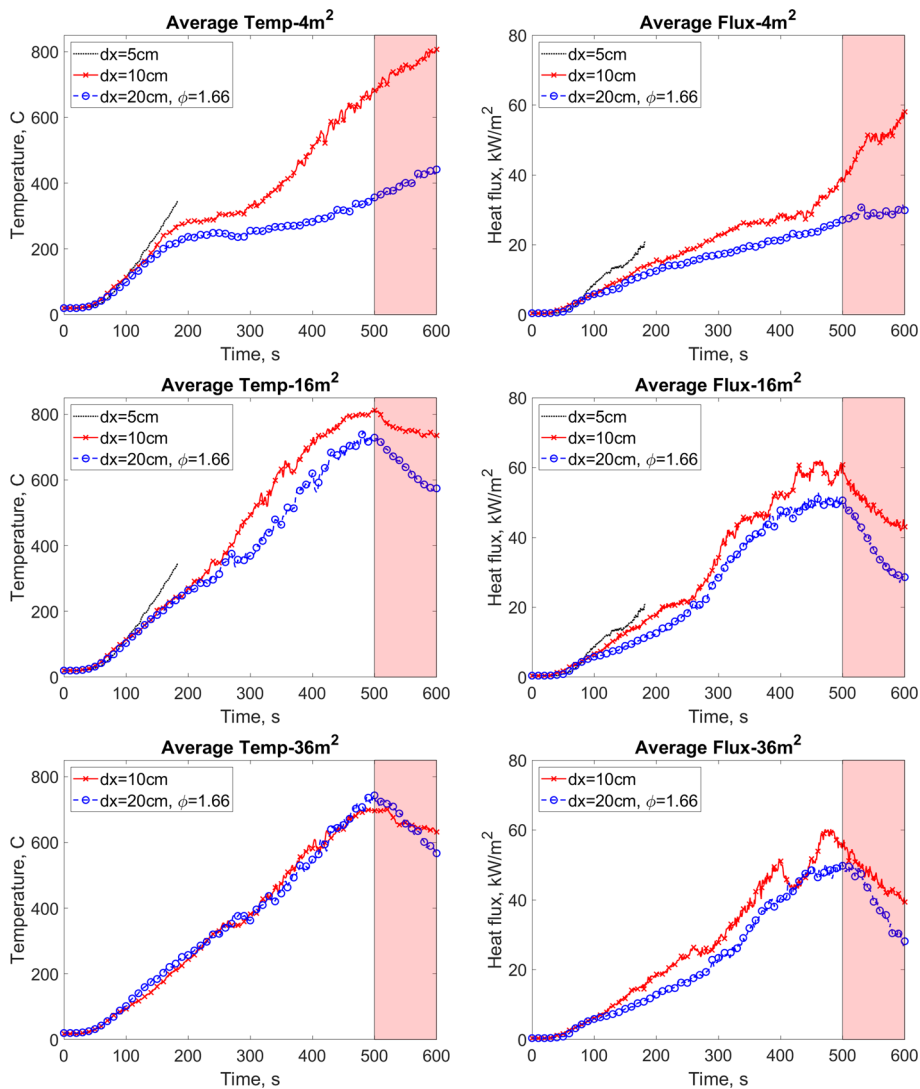
**Figure 13. Average temperature and heat flux recorded with prescribed areas 4 m², 16 m² and 36 m² with 10 cm and 20 cm grid resolutions. Area adjust of 1.66 is applied to the 20 cm simulations.**

domain boundaries. After this time (500 s), the output quantities, including HRR, are not reliable because as the flames extend beyond the computational domain (as shown in Fig. 10), the energy produced cannot be accounted completely.

### 4.3. Discussion

The predicted fire spread was found to depend both on the grid resolution and the size of the prescribed fire source. Beyond the prescribed region, the fire spread, as indicated by HRR, in 20 cm simulations was slower than in the 10 cm simulations. The accuracy of the coarse mesh simulations was vastly improved by the area adjustment except for the 4 m$^2$ prescribed region, where the energy from the initial fire was not sufficient to produce a consistent fire spread. The lack of fire spread on a 20 cm mesh for the 4 m$^2$ case shows that we are unable to accurately resolve the flame temperatures in the initial region. Fire spread was observed to occur consistently across different grid resolutions with a prescribed area of 16 m$^2$. This supports our hypothesis that the consistent room scale fire spread simulations can be carried out even with coarse resolutions if the initial fire is sufficiently large.

Next we would like to know if there is an optimal size of the initial fire region. Table 5 presents the times at which the fire front reaches the edge of a prescribed region together with the times of first ignition in the predicted region. While the former times increase with region size (constant fire spread velocity), the latter times are found to vary much less. For the 10 cm resolution, the predicted region ignites in 120...148 s, i.e. before the fire front has reached it. With the 20 cm resolution, the predicted ignitions occur at the same time or earlier than the fire spread time would indicate. Assuming that the ignition times at different distances from the centre should be monotonically increasing, we can conclude that the 4 m$^2$ prescribed region is slightly too large for the 10 cm simulations but suitable for 20 cm resolution. Correspondingly, the 16 m$^2$ and 36 m$^2$ regions are limiting the HRR development at both resolutions. These events are also visible in Fig. 14 showing the instantaneous burning rates from the 20-cm resolution simulations with the two prescribed regions. Prescribed burning areas are seen as circles inside the square-shaped prescribed regions, while predicted regions have just ignited.
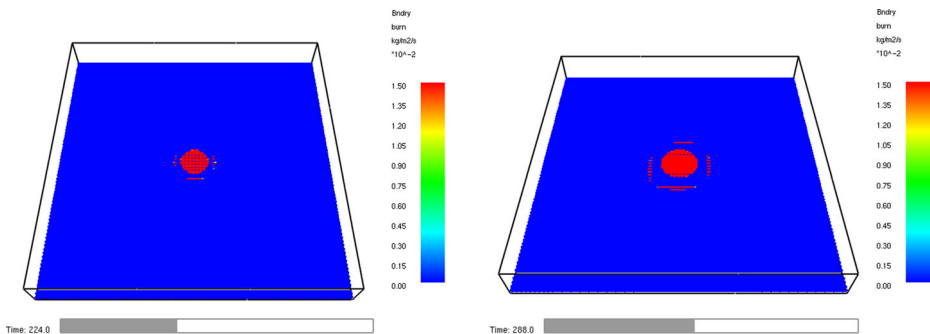


**Figure 14. Instantaneous burning rate at the time of predicted ignitions with 20 cm grid resolution and area adjust 1.66 for the prescribed areas 16 m$^2$ (left) and 36 m$^2$ (right).**

**Table 5**
**Time Taken by the Fire to Reach the Edge of a Prescribed Area, Time to Reach the Predicted Region and Time to Reach a HRR Threshold of 100 MW Under Different Grid Resolutions**

| Prescribed area ($m^2$) | Time to the edge of prescribed region (s) | | | Time of ignition in predicted region (s) | | | Time to HRR threshold (s) | | |
|---|---|---|---|---|---|---|---|---|---|
| | 5 cm | 10 cm | 20 cm | 5 cm | 10 cm | 20 cm | 5 cm | 10 cm | 20 cm |
| 4 | 188 | 145 | 141 | 100 | 120 | 142 | – | 500 | – |
| 16 | 376 | 289 | 282 | – | 140 | 224 | – | 383 | 443 |
| 36 | – | 433 | 423 | – | 148 | 288 | – | 420 | 457 |

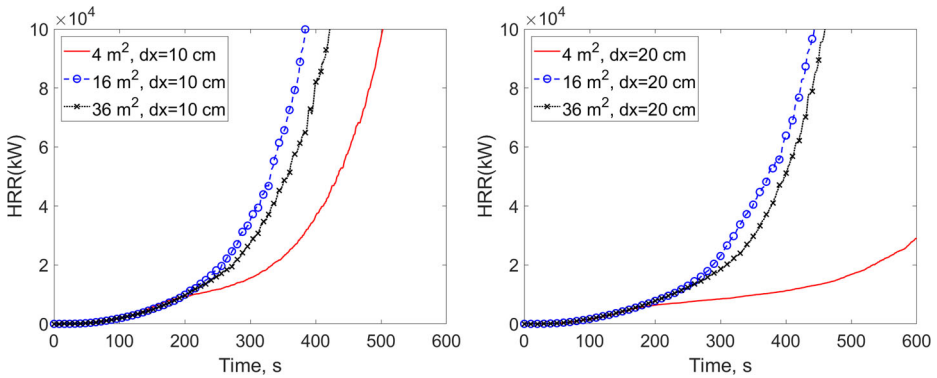The 20 cm results were computed with area adjustment



**Figure 15. Comparison of heat release rates for different prescribed areas for 10 cm and 20 cm grid resolutions. The fastest fire spread was observed with the 16 $m^2$ initial fire area.**

HRR predictions with three prescribed regions are compared in Fig. 15 for the 10 cm and 20 cm resolutions. For the first 200 s, during which the diameter of the burning circle increases to about 2.8 m, the HRR curves are identical. After the first 200 s, we observe that increasing the prescribed region from 4 $m^2$ to 16 $m^2$ increases the growth rate, but increasing it further to 36 $m^2$ actually slows down the fire growth. In the light of these results, optimal prescribed area size is somewhere between 4 $m^2$ and 16 $m^2$ for the 10 cm resolution, and around 16 $m^2$ for the 20 cm resolution. These results are slightly contradictory to the conclusions based on the region timings. From the viewpoint of the large-scale fire development, the robustness of the HRR predictions beyond the prescribed region can be regarded more important, and the HRR errors due to the region boundary timings (Table 5) may be insignificant.

Qualitatively, the phenomena shown in Fig. 14 can be seen as far-field ignitions resulting from the radiative heat feedback from the flames, hot gas layer and ceiling jet to the wood cribs. To ensure the relevance of the conclusions regarding the

fire spread predictions, it is important to ensure that these far field ignitions are still mainly related to the fire plume above the burning region, and not to the global room scale events such as flashover. Using the empirical correlations in [35], we can estimate that the critical HRR for flashover is between 74 MW (McCaffrey's correlation) and 620 MW (Babrauskas' correlation). Choosing a critical HRR of 100 MW, we can estimate the times when the simulations would lead to global ignition. These times are shown in the right-most columns of Table 5. As they are significantly longer than the observed far-field ignitions, we can conclude that the heat transfer modes leading to the observed far-field ignitions are relevant for fire spread.

To generalize, we can conclude that prescribing a larger area than necessary can lead to delayed fire spread because a sustained ignition of the predicted fire load may not occur until the prescribed fire front reaches it. The situation is analogous to a scenario where there is a gap between isolated fire loads. The optimum area of prescribed fire would be the smallest area which produces fastest, sustained fire spread across different grid resolutions. In our case, the area was quite large as the compartment was modelled with open boundaries.

It was observed that the fire had a preferential direction of propagation after the prescribed region, resulting in an asymmetric fire field as shown in the Fig. 10. The direction of propagation was dependent on the channels created by wood sticks at the bottom of the room. This phenomenon is elaborated in Fig. 16 showing instantaneous burning rate and flame location 436 s after ignition in the case with 16 m$^2$ prescribed region. This effect was more distinct and had a significant influence on fire spread in the simulation with 10 cm resolution. This effect may be eliminated when the fire load is not uniformly distributed.

A comparison between the SP and room scale fire simulations reveals an interesting aspect: The room scale simulations required us to prescribe an initial area for fire spread whereas the SP simulations did not need an initial prescribed fire. In the SP simulations, an ignitor was enough to produce fire spread as the wood cribs were calibrated to produce necessary energy. On the other hand, the room
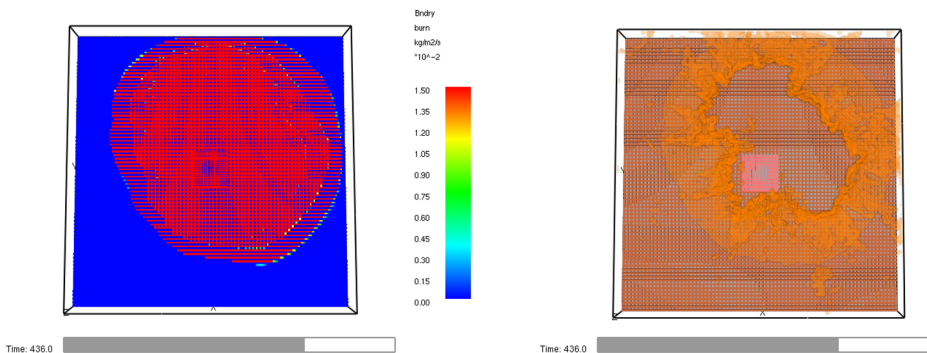


**Figure 16.** **Preferential propagation of fire in the 10 cm grid simulation with a prescribed area of 16 m$^2$. Burning rate on the left, flame visualization on the right.**

scale simulations did not have any calibrations, hence a prescribed region was necessary to model a consistent fire spread scenario.

The chosen ignition temperature model predicts the fire behaviour well but is limited due to its inability to adjust the burning rate when solid fuel cools below the pyrolysis temperature. In this type of model, the mass flux from a fuel surface continues until the combustible mass of the cell is exhausted. This means the model does not respond to a lack of ventilation. Also, char formation and the subsequent decrease in fuel burning rate are not accounted for.

## 5. Conclusion

The objectives of this study were to validate the use of ignition temperature model accompanied by area adjust for coarse mesh fire spread simulations and to perform room scale fire spread simulations reliably. The fine mesh simulations of the SP tunnel tests were able to reproduce the experimental results with only 1% bias. In the coarse mesh simulations, the peak HRR was under-predicted and fire growth rates were delayed in a few cases. Applying the proposed correction to the fuel surface area improved the prediction of both peak HRR and fire growth rates, enabling more than 80% reduction of CPU time.

In the room scale fire spread simulations, the grid resolution affected the HRR predictions considerably, but the use of area adjust in coarse-mesh computations brought the results closer to the fine-mesh HRR predictions. Consequently, the CPU times reduced from 44 h to approximately 10 h. An initial area of 16 $m^2$ with prescribed fire spread was needed to produce consistent fire spread with this particular room configuration and fire load distribution. Coarse-mesh temperatures and heat fluxes converged towards the fine-mesh results as well, when the area of prescribed fire was increased.

The results showed that the computational cost of the fire spread simulations can be reduced by using coarser meshes and sufficient accuracy can be maintained by using the area adjust parameter. The applicability of the specific fire size and resolution requirements to other compartment configurations may not be straightforward, but the proposed principle can certainly be genaralized.

These findings form the basis for future research we intend to conduct using more detailed wood pyrolysis model along with the area adjust parameter. The effects of the compartment boundaries, ventilation and different fire load distributions will also be investigated as these parameters have a significant influence on the direction of fire spread and the fire duration.

## Acknowledgements

son and Dr. Rickhard Hansen for providing us with test data for the tunnel fire tests.

## Open Access

This article is distributed under the terms of the Creative Commons Attribution 4.0 International License (http://creativecommons.org/licenses/by/4.0/), which permits unrestricted use, distribution, and reproduction in any medium, provided you give appropriate credit to the original author(s) and the source, provide a link to the Creative Commons license, and indicate if changes were made.

## References

1. Babrauskas V, Williamson RB (1978) The historical basis of fire resistance testing—part 2. Fire Technol 14(4):301–316
2. Petterson O, Magnusson SE, Thor J (1976) Fire engineering design for steel structures. Swedish Institute of Steel Construction,  Stockholm
3. Eurocode 1: Actions on Structures-Part 1-2: General Actions–Actions on Structures Exposed to Fire, European Standard EN 1991-1-2, European Committee for Standardization, Brussels, 2002
4. Blagojevic MD, Pesic DJ (2012) A new curve for temperature time relationship in compartment fire. Therm Sci 15(2):339–352
5. Du G, Li G-Q (2012) A new temperature time curve for fire resistance analysis of structures. Fire Saf J 51:113–120
6. Zhongcheng M, Makelainen P (2000) Parametric temperature time curves of medium compartment fires for structural design. Fire Saf J 34:361–375
7. Lennon T, Moore D (2003) The natural fire safety conceptfull-scale tests at Cardington. Fire Saf J 38(7):623–643. https://doi.org/10.1016/S0379-7112(03)00028-6
8. Stern-Gottfried J, Rein G (2012) Travelling fires for structural design—part I: literature review. Fire Saf J 54:74–85
9. Stern-Gottfried J, Rein G (2012) Travelling fires for structural design—part II: design methodology. Fire Saf J 54:96–112
10. Horová K, Wald F, Bouchair A (2013) Travelling fire in full-scale experimental building. In: Jármai K, Farkas J (eds) Design, fabrication and economy of metal structures. Springer, Berlin, pp 371–376
11. Hankalin V, Ahonen T, Raiko R (2009) On thermal properties of a pyrolysing wood particle. Finnish-Swedish Flame Days
12. Lukosius A, Vekteris V (2003) Precision of heat release rate measurement results. Meas Sci Rev 3(3):12–16
13. Rush D, Lange D, Maclean J, Rackauskaite E (2015) Effects of a travelling fire on a concrete columns—Tisova fire test. Paper presented at Applications of Structural Fire Engineering, Dubrovnik, Croatia
14. Tanaka T (1983) A model of multiroom fire spread. Fire Sci Technol 3:105–121. https://doi.org/10.3210/fst.3.105
15. Ling W-CT, Williamson RB (1985) Modeling of fire spread through probabilistic networks. Fire Saf J 9(3):287–300. https://doi.org/10.1016/0379-7112(85)90039-6

16. Ramachandran G (1991) Non-deterministic modelling of fire spread. J Fire Prot Eng 3:37–48
17. Platt DG, Elms DG, Buchanan AH (1994) A probabilistic model of fire spread with time effects. Fire Saf J 22(4):367–398. https://doi.org/10.1016/0379-7112(94)90041-8
18. Cheng H, Hadjisophocleous GV (2009) The modeling of fire spread in buildings by Bayesian network. Fire Saf J 44(6):901–908. https://doi.org/10.1016/j.firesaf.2009.05.005
19. Bryner N, Madrzykowski D, Grosshandler W (2007) Reconstructing the station night-club fire—computer modeling of the fire growth and spread. In: Proceedings of the 11th international interflam conference, 3–5 September 2007. Interscience Communications, London, pp 1181–1192
20. Galea ER, Wang Z, Veeraswamy A, Jia F, Lawrence PJ, Ewer J (2008) Coupled fire/evacuation analysis of the station nightclub fire. Fire Saf Sci 9:465–476
21. Chen CJ, Hsieh WD, Hu WC, Lai CM, Lin TH (2010) Experimental investigation and numerical simulation of a furnished office fire. Build Environ 45(12):2735–2742
22. Yang P, Tan X, Xin W (2011) Experimental study and numerical simulation for a storehouse fire accident. Build Environ 46(7):1445–1459. https://doi.org/10.1016/J.BUILDENV.2011.01.012
23. Ahn CS, Kim JY (2011) A study for a fire spread mechanism of residential buildings with numerical modeling. WIT Trans Built Environ 117:185–196. https://doi.org/10.2495/SAFE110171
24. Shu S-B, Chuah YK, Lin C-J (2012) A study on the spread of fire caused by the stack effects of patio—a computer modeling and a reconstruction of a fire scenario. Build Simul 5(2):169–178
25. Chi J-H (2013) Reconstruction of an inn fire scene using the fire dynamics simulator (FDS) program. J Forensic Sci 58:S1
26. Meunders A, Baker G, Arnold L, Schröder B, Spearpoint M, Pau D (2014) Parameter optimization and sensitivity analysis for fire spread modelling with FDS. In: International conference on performance-based codes and fire safety
27. Cheong MK, Spearpoint MJ, Fleischmann CM (2009) Calibrating an FDS simulation of goods-vehicle fire growth in a tunnel using the Runehamar experiment. J Fire Prot Eng 19(3):177–196. https://doi.org/10.1177/1042391508101981
28. Hansen R, Ingason H (2012) Heat release rates of multiple objects at varying distances. Fire Saf J 52:1–10
29. Hansen R, Ingason H (2010) Model scale fire experiments in a model tunnel with wooden pallets at varying distances. Studies in Sustainable Technology 2010:08. Mälardalen University
30. McGrattan K, McDermott R, Floyd J, Hostikka S, Forney G, Baum H (2012) Computational fluid dynamics modelling of fire. Int J Comput Fluid Dyn 26:349–361
31. McGrattan K, Hostikka S, McDermott R, Floyd J, Vanella M (2017) Fire dynamics simulator, technical reference guide. Volume 1: mathematical model. National Institute of Standards and Technology, Gaithersburg, Maryland, USA, and VTT Technical Research Centre of Finland, Espoo, Finland. NIST Special Publication 1018-1. 6th edition, November
32. McGrattan K, Hostikka S, McDermott R, Floyd J, Vanella M (2017) Fire dynamics simulator, validation guide. Volume 3: validation. National Institute of Standards and Technology, Gaithersburg, Maryland, USA, and VTT Technical Research Centre of Finland, Espoo, Finland. NIST Special Publication 1018-3. 6th edition, November
33. Hietaniemi J, Mikkola E (2010) design fires for fire safety engineering. In: VTT working papers 139. VTT, Technical Research Centre of Finland. February

34. Hurley MJ( (2016) SFPE handbook of fire protection engineering, 5th edn. Springer, New York
35. Drysdale D (2013) An introduction to fire dynamics, 3rd edn. Wiley, West Sussex
36. Quintiere JG (2016) Principles of fire behavior, 2nd edn. CRC Press, Boca Raton